RSC Advances

PAPER

View Article Online
View Journal | View Issue

Cite this: *RSC Adv.*, 2021, **11**, 34338

Expanded scope of Griesbaum co-ozonolysis for the preparation of structurally diverse sensors of ferrous iron†

Jun Chen, Ryan L. Gonciarz and Adam R. Renslo *

Received 5th August 2021
Accepted 11th October 2021

DOI: 10.1039/d1ra05932g

rsc.li/rsc-advances

Sterically shielded 1,2,4-trioxolanes prepared by Griesbaum co-ozonolysis have been utilized as chemical sensors of ferrous iron in several recently described chemical probes of labile iron. Here we report optimized conditions for co-ozonolysis that proceed efficiently and with high diastereoselectivity across an expanded range of substrates, and should enable a new generation of labile iron probes with altered reaction kinetics and physicochemical properties.

In the mid-1990s,[1] Griesbaum and co-workers reported the co-ozonolysis of ketone and ketoxime reactants for the preparation of unsymmetrically substituted 1,2,4-trioxolanes. When cyclic ketone and oxime co-reactants are employed in this process, the resulting trioxolane adducts can be remarkably stable due to shielding of the endoperoxide bond by proximal axial C–H bonds of the surrounding carbocyclic ring systems. Vennerstrom and co-workers exploited this reaction and the shielding effect of the rigid adamantane ring system to develop the antimalarial agents arterolane[2] (Fig. 1) and artefenomel.[3] The hindered endoperoxide embedded within their structures, like that in the 1,2,4-trioxane ring of artemisinin derivatives, confers an antimalarial effect *via* initial Fenton-type reaction with unbound, or "labile", ferrous iron sources in the parasite.

Increasing appreciation for the importance of labile iron as the bioavailable pool of iron in cells has motivated the development of chemical probes capable of detecting iron with oxidation-state specificity.[4] Detection of ferrous iron has been achieved largely through reactivity-based approaches[4c,d] in which ferrous iron promotes the reduction of N–O or O–O bonds to activate a fluorophore (*e.g.* SiRhoNox[5] and related analogs[6]), separate a FRET pair (*e.g.*, TRX-FRET,[7] FIP-1 (ref. 8)), release a tethered reporter payload (*e.g.*, TRX-PURO,[7] ICL-1,[9] HNG[10]), or covalently sequester a PET radionuclide in cells/tissues of animals (^{18}F-TRX[11,12]). Trioxane and trioxolane-based reagents have also been employed for chemoproteomic studies of the malaria parasite[13] and of mammalian cancer cells (FIPC-1 (ref. 14)). Whilst an arterolane-like pharmacophore has figured prominently in many of these first-generation probes, their further development and optimization is likely to require access to trioxolane systems exhibiting a broader range of iron reactivities and enhanced physiochemical properties for *in vivo* applications. We therefore reinvestigated the Griesbaum co-ozonolysis with the aim of enabling new structural architectures of potential utility for ferrous iron-reactive therapeutics and chemical probes.

The Griesbaum co-ozonolysis proceeds *via* [3 + 2]/retro-[3 + 2] reaction of the oxime reactant with ozone to afford a carbonyl oxide intermediate. This species then reacts with the ketone component in a final, stereochemistry determining [3 + 2] cycloaddition to afford 1,2,4-trioxolane adducts. The reaction of adamantane oximes with substituted cyclohexanones is known to proceed selectively *via* axial addition of carbonyl oxide to ketone, affording *cis*-4′ or *trans*-3′ adducts with useful (~9 : 1 d.r.) diastereoselectivity (Scheme 1).[15] The seminal reports from Griesbaum described mostly undecorated alkyl and cycloalkyl substrates, whereas more recent work[7,8,14,16] has focused on the adamantane oximes that were found to yield pharmacologically active products, though other groups have explored reactions of non-adamantane substrates.[17–19] We previously reported[15] an optimized protocol to access 3′-hydroxy adducts useful for drug and reporter payload delivery in an iron(II)-dependent fashion. This protocol involved use of the ketone component as limiting

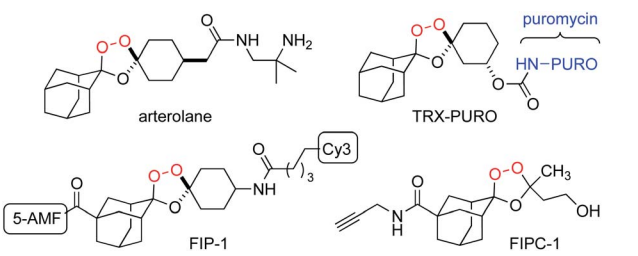

Fig. 1 Structures of recently described probes of ferrous iron employing a 1,2,4-trioxolane-based sensor of ferrous iron, inspired by the synthetic antimalarial arterolane.

Department of Pharmaceutical Chemistry, University of California, San Francisco, San Francisco, California, 94143, USA. E-mail: adam.renslo@ucsf.edu

† Electronic supplementary information (ESI) available. See DOI: 10.1039/d1ra05932g

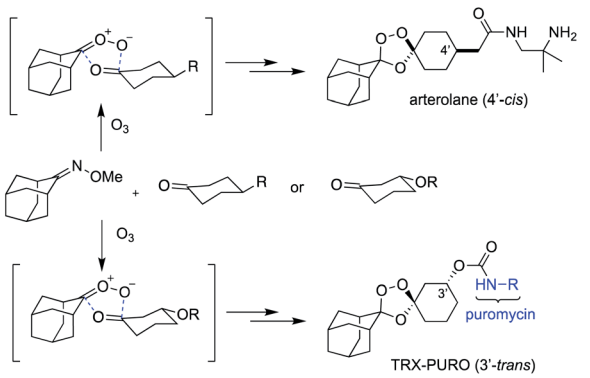

Scheme 1 Griesbaum co-ozonolysis proceeds *via* conversion of the oxime to carbonyl oxide, followed by diastereoselective reaction with the ketone co-reactant, with axial addition favored, as shown.

reagent, and proceeds in good yields (~70%) with adamantane oxime at 0 °C in CCl_4. Unfortunately, we have since found these conditions to be unsatisfactory when applied to substituted adamantanes, and particularly to non-adamantyl systems, with yields often in the range of 5–23% and in some cases failing altogether to afford the desired adducts.

We hypothesized that side-reactions of ozone and/or the highly reactive carbonyl oxide intermediate[20] may have contributed to poor yields with certain substrates. To explore this possibility, we evaluated the reaction of enantiopure ketone **2** (ref. 21) with a variety of substituted adamantanone oxime substrates under low temperature conditions reported previously[19] for a different substrate (Table 1). We were pleased to find that reactions of **2** with various oximes (3 equiv.) at −78 °C in hexanes, using an oxygen flow rate = 1.1 liters per minute, or 6 g h^{-1} O_3, afforded modest (50% for **3b**) to excellent (77–94% for **3a**, and **3c–3e**) isolated yields of the desired adducts (Table 1). Our previous conditions afforded adduct **3a** in variable yields ranging from 91% (ref. 21) to as low as 48%, while substituted adducts **3b–3e** were obtained in only very poor yield (Table 1). Notably, the diastereofacial selectivity of the final [3 + 2] cycloaddition is further improved under the low temperature conditions. Thus, adducts **3a–3e** were formed as a single *trans* diastereomer, as shown, whereas ~10% of the *cis* diastereomer is formed under the original conditions (see ESI† for NMR spectra). As was expected, little diastereofacial selectivity is observed with respect to unsymmetrical carbonyl oxides during

Table 1 Isolated yields of trioxolane adducts obtained under either conventional reaction condition A (in CCl_4, 0 °C) or low temperature condition B (in hexane, −78 °C)

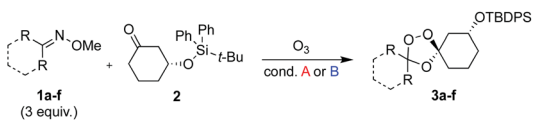

	Product (**3a–f**)	A: CCl_4, 0 °C	B: hexane, −78 °C
3a	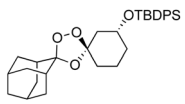	48–91%	91%
3b	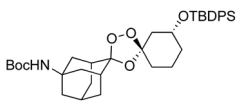	28%[a]	50%
3c	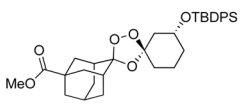	23%	77%
3d	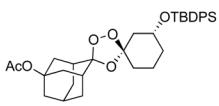	5%	85%
3e	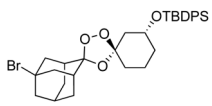	18%	94%
3f	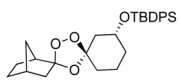	0%	81%

[a] Calculated yield based on ^{1}H NMR.

Table 2 Scope of Griesbaum co-ozonolysis involving structurally diverse oximes **1** and ketone **2** under low temperature conditions

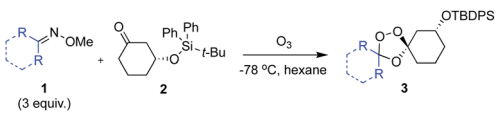

Product (**3f–k**)	Isolated yield	Product (**3l–q**)	Isolated yield
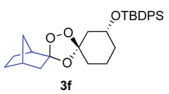	70–82%	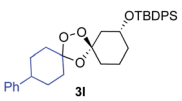	75%
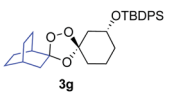	26–44%	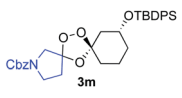	0%
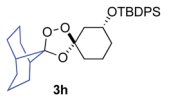	80–87%	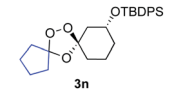	0%
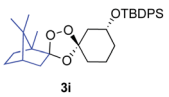	0%	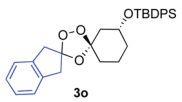	0%
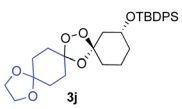	71%	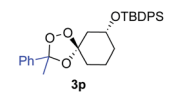	0%
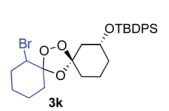	53%	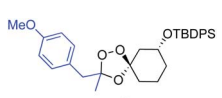	4%

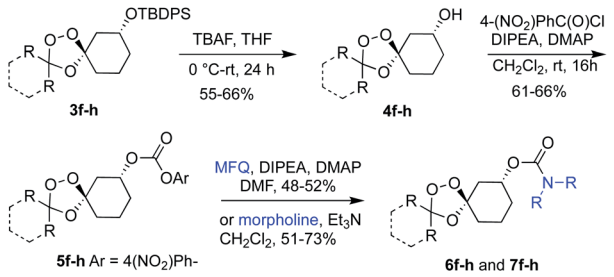

Scheme 2 Synthesis of mefloquine and morpholine conjugates **6f–h** and **7f–h** from intermediates **3f–h**. MFQ = mefloquine, an antimalarial drug with a secondary amine function serving as the site of conjugation.

the [3 + 2] cycloaddition (note that only one of the two diastereomers of **3b–3e** is shown Table 1).

As noted above, the Fenton-type, iron(II)-specific reactivity of reporter-based probes like TRX-PURO and ICL-1 is modulated by the axial C–H bonds surrounding the endoperoxide function.[22] To evaluate the potential of other aliphatic bicyclic ring systems to similarly shield the endoperoxide function, we computed minimized conformations of several potential adducts using MarvinSketch software (see ESI, Fig. S1†). From this analysis, we selected the bicyclo[2.2.1]heptane, bicyclo [2.2.2]octane, and bicyclo[3,3,1]nonane ring systems as likely to produce trioxolane adducts with desirable iron reactivity kinetics. Using low temperature reaction condition B, we were pleased to find that co-ozonolysis of **2** with bicyclo[2.2.1]heptan-2-one methyl oxime provided the desired adduct **3f** in 81% isolated yield as a mixture of stereoisomers that were partially resolved by ^{1}H NMR (three distinct resonances in a 13 : 8 : 1 ratio). The same reaction failed to afford any isolable amount of **3f** under condition A (Table 1).

Buoyed by the successful generation of **3f**, we explored the co-ozonolysis of additional oxime substrates under low temperature conditions (Table 2). Thus, reaction of **2** with bicyclo[2.2.2]octan-2-one methyl oxime or bicyclo[3.3.1]nonan-9-one methyl oxime afforded the desired adducts **3g** and **3h** in modest (26–44%) and excellent (80–87%) yields, respectively. The methyl oxime of camphor failed to afford adduct **3i**, perhaps due to a more hindered steric environment around the oxime. Substituted cyclohexyl, cyclopentyl, and acyclic oximes were also investigated as substrates in the process. Cyclohexan-1-one oximes substituted at the 4-position afforded the desired adducts **3j** (71%) and **3l** (75%) in good yields, while 2-bromocyclohexan-1-one methyl oxime afforded **3k** in 53% yield. Unexpectedly, cyclopentanone oxime substrates failed to yield isolable quantities of the expected adducts **3m**, **3n**, and **3o**. It is possible that the failure of these reactions reflects instability of the trioxolane adducts, or competing reactions of the carbonyl oxide (*e.g.*, dimerization). Similarly, the methyl oximes of acetophenone and 4-methoxyphenylacetone failed to afford useful yields of the expected adducts **3p** and **3q**.

Next, we sought to evaluate the Fe^{2+} reactivity of novel adducts like **3f**, **3g**, and **3h** in the context of payload bearing trioxolane conjugates. Using conditions described previously by our group[23] for the conversion of **3a** to the mefloquine conjugate TRX-MFQ, **3f–3h** were similarly converted to iron(II)-sensitive conjugates of mefloquine (MFQ) and morpholine (Scheme 2). Hence, intermediates **3f–h** were treated with TBAF in THF to afford the alcohols **4f–h**, which were then converted immediately to the *para*-nitrophenyl carbonate intermediates **5f–h** before a final coupling with either mefloquine to afford **6f–h** or morpholine to afford **7f–h** (Scheme 2).

As a surrogate measure of Fe^{2+} reactivity under physiological conditions, and to evaluate their ability to undergo iron(II)-dependent payload release, we evaluated **6f–h** and **7f–h** along

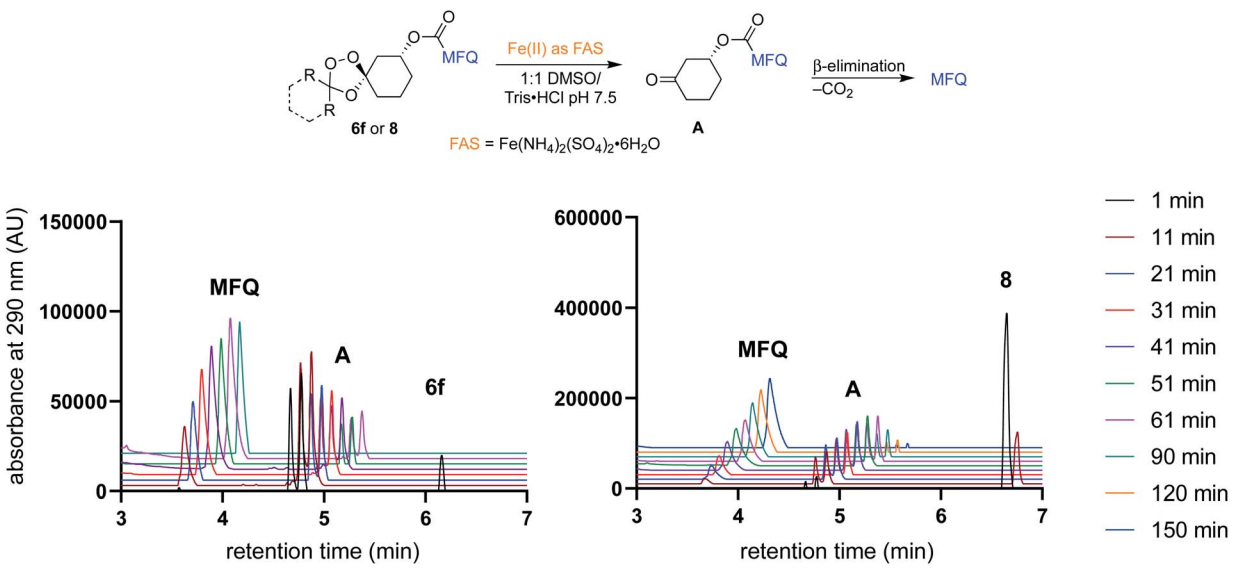

Fig. 2 *In vitro* iron fragmentation studies of the previously described, *in vivo* efficacious mefloquine conjugate **8** and the new congener **6f** bearing a bicyclo[2.1.1]heptane ring in place of the adamantane. Fragmentation of the trioxolane with FAS is rapid for both conjugates, with β-elimination from common intermediate **A** being the rate limiting step in mefloquine (MFQ) release.

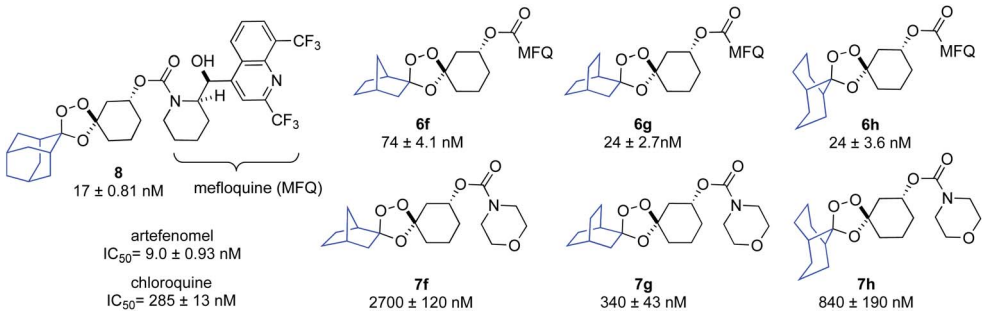

Chart 1 *In vitro* antiplasmodial activity of **6f–h**, **7f–h** and the known conjugate **8** against W2 *P. falciparum* parasites ($IC_{50} \pm$ SEM). Reported IC_{50} values are the means of at least three determinations. IC_{50} values for artefenomel and chloroquine controls are indicated at bottom left. The superior potency of conjugates **6** *vs.* **7** imply their activity is derived from mefloquine (MFQ) release.

with TRX-MFQ[23] (**8**) as positive control, for activity against cultured *P. falciparum* parasites (W2 strain) using a standard protocol (Chart 1).[24] Mefloquine bearing conjugates **6f–h** exhibited potent IC_{50} values of 74 nM (for **6f**) and 24 nM (**6g** and **6h**), which were similar to that of the positive control **8** (IC_{50} = 17 nM). By contrast, morpholine-bearing conjugates **7f–h** were markedly less potent, with IC_{50} values between 340 and 2700 nM (Chart 1), which is some 10–100 fold weaker than observed previously for congeneric adamantane-derived trioxolane comparators with a morpholine side chain.[21] Accordingly, the potent anti-plasmodial activities of **6f–h** can be inferred to result from iron(II)-dependent activation and release of the mefloquine payload by the canonical mechanism[7,25] of payload release from "TRX" conjugates.

To further study the kinetics and regioselectivity of iron(II)-dependent activation, we followed the reaction of **6f** and **8** with ferrous ammonium sulfate by UPLC/MS. As we have described previously for the progenitor TRX moiety,[7,25] efficient activation and payload release requires regioselective activation of the endoperoxide bond by Fe^{2+} such that the ketone intermediate **A** is produced preferentially over the alternative adamantan-2-one product (Fig. 2). In adamantane-based systems this regioselectivity is conferred by the steric effect of the adamantane ring, as noted previously.[22] We predicted based on modeling that the bicyclo[2.2.1]heptane moiety of **6f** should similarly shield the proximal oxygen atom from inner-sphere coordination with Fe^{2+} leading to regioselective peroxide scission. In the event, exposure of either **6f** or **8** to Fe^{2+} (as ferrous-ammonium sulfate with pH 7.4 Tris buffer) led within minutes to clean conversion to the common cyclohexanone intermediate **A** (Fig. 2). No detectable quantity of the alternate bicyclo[2.2.1]heptan-2-one product was detected in the reactions of **6f**, thus confirming that the process is highly regioselective. Conversion of **6f** to **A** was moderately faster than for comparator **8**, with **6f** fully consumed by the 11 minute time point. The kinetics of mefloquine release from intermediate **A** were comparable within experimental error. Taken together, the antiplasmodial and cell-free Fe^{2+} reactivity data indicate that efficient iron(II)-dependent uncaging and traceless release of payloads can be realized from non-adamantane based scaffolds such as **6f** and likely as well from the other scaffolds described herein.

Conclusions

In summary, we explored the scope of Griesbaum co-ozonolysis under optimized low temperature reaction conditions. Overall, these conditions afford improved yields, substrate scope, and diastereoselectivity as compared to our previously described conditions. Highly hindered ketoximes remain problematic substrates, while trioxolane adducts lacking a sufficiently shielded endoperoxide bond are likely unstable to isolation. However, with the appropriate selection of ketoxime and ketone reactants, a variety of new adducts could be prepared using the improved conditions. Three of these new adducts were conjugated to drug or control payloads and shown in antiplasmodial assays and chemical Fe^{2+} reactivity studies to be competent sensors of ferrous iron, much like the parental TRX system.

These findings are significant insofar as they should enable iron(II)-activated chemistries to be applied to a broader range of drug or reporter payloads whilst maintaining physiochemical properties and iron(II)-dependent reactivity within a pharmacologically desirable range. As such, our findings have implications for antimalarial drug discovery, iron(II)-dependent drug delivery, and the continuing development of new chemical tools to study labile ferrous iron in biological settings.

Author contributions

All authors participated in the design of experiments, interpretation of data, and writing the manuscript. J. Chen and R. Gonciarz performed experiments. A. R. Renslo supervised research.

Conflicts of interest

The authors declare the following competing financial interest(s): A. R. R. is an advisor and co-founder of Tatara Therapeutics.

Acknowledgements

A. R. R. acknowledges funding from National Institutes of Health grant AI105106 and Congressionally Directed Medical Research Program, grants W81XWH1810763 and

W81XWH1810754. We thank Jennifer Legac (UCSF) for anti-malarial testing of analogues **6f–h** and **7f–h**.

Notes and references

1 (*a*) K. Griesbaum, X. Liu, A. Kassiaris and M. Scherer, *Liebigs Ann.*, 1997, **1997**, 1381; (*b*) K. Griesbaum, B. Övez, T. S. Huh and Y. Dong, *Liebigs Ann.*, 1995, **1995**, 1571.

2 J. L. Vennerstrom, S. Arbe-Barnes, R. Brun, S. A. Charman, F. C. K. Chiu, J. Chollet, Y. Dong, A. Dorn, D. Hunziker, H. Matile, K. McIntosh, M. Padmanilayam, J. Santo Tomas, C. Scheurer, B. Scorneaux, Y. Tang, H. Urwyler, S. Wittlin and W. N. Charman, *Nature*, 2004, **430**, 900.

3 S. A. Charman, S. Arbe-Barnes, I. C. Bathurst, R. Brun, M. Campbell, W. N. Charman, F. C. K. Chiu, J. Chollet, J. C. Craft, D. J. Creek, Y. Dong, H. Matile, M. Maurer, J. Morizzi, T. Nguyen, P. Papastogiannidis, C. Scheurer, D. M. Shackleford, K. Sriraghavan, L. Stingelin, Y. Tang, H. Urwyler, X. Wang, K. L. White, S. Wittlin, L. Zhou and J. L. Vennerstrom, *Proc. Natl. Acad. Sci. U. S. A.*, 2011, **108**, 4400.

4 (*a*) A. T. Aron, A. G. Reeves and C. J. Chang, *Curr. Opin. Chem. Biol.*, 2018, **43**, 113; (*b*) C. J. Chang, *Nat. Chem. Biol.*, 2015, **11**, 744; (*c*) K. J. Bruemmer, S. W. M. Crossley and C. J. Chang, *Angew. Chem., Int. Ed.*, 2020, **59**, 13734; (*d*) T. Hirayama, *Free Radical Biol. Med.*, 2019, **133**, 38.

5 T. Hirayama, H. Tsuboi, M. Niwa, A. Miki, S. Kadota, Y. Ikeshita, K. Okuda and H. Nagasawa, *Chem. Sci.*, 2017, **8**, 4858.

6 T. Hirayama, A. Miki and H. Nagasawa, *Metallomics*, 2018, **11**, 111.

7 B. Spangler, C. W. Morgan, S. D. Fontaine, M. N. Vander Wal, C. J. Chang, J. A. Wells and A. R. Renslo, *Nat. Chem. Biol.*, 2016, **12**, 680.

8 A. T. Aron, M. O. Loehr, J. Bogena and C. J. Chang, *J. Am. Chem. Soc.*, 2016, **138**, 14338.

9 A. T. Aron, M. C. Heffern, Z. R. Lonergan, M. N. Vander Wal, B. R. Blank, B. Spangler, Y. Zhang, H. M. Park, A. Stahl, A. R. Renslo, E. P. Skaar and C. J. Chang, *Proc. Natl. Acad. Sci. U. S. A.*, 2017, **114**, 12669.

10 S. Xu, H.-W. Liu, L. Chen, J. Yuan, Y. Liu, L. Teng, S.-Y. Huan, L. Yuan, X.-B. Zhang and W. Tan, *J. Am. Chem. Soc.*, 2020, **142**, 2129.

11 N. Zhao, Y. Huang, Y. H. Wang, R. K. Muir, Y. C. Chen, N. Hooshdaran, J. Wei, P. Viswanath, Y. Seo, D. Ruggero, A. R. Renslo and M. J. Evans, *J. Nucl. Med.*, 2021, **62**, 949.

12 R. K. Muir, N. Zhao, J. Wei, Y.-h. Wang, A. Moroz, Y. Huang, Y.-C. Chen, R. Sriram, J. Kurhanewicz, D. Ruggero, A. R. Renslo and M. J. Evans, *ACS Cent. Sci.*, 2019, **5**, 727.

13 (*a*) H. M. Ismail, V. E. Barton, M. Panchana, S. Charoensutthivarakul, G. A. Biagini, S. A. Ward and P. M. O'Neill, *Angew. Chem., Int. Ed.*, 2016, **55**, 6401; (*b*) C. Wei, C.-X. Zhao, S. Liu, J.-H. Zhao, Z. Ye, H. Wang, S.-S. Yu and C.-J. Zhang, *Chem. Commun.*, 2019, **55**, 9535.

14 Y.-C. Chen, J. A. Oses-Prieto, L. E. Pope, A. L. Burlingame, S. J. Dixon and A. R. Renslo, *J. Am. Chem. Soc.*, 2020, **142**, 19085.

15 S. D. Fontaine, A. G. DiPasquale and A. R. Renslo, *Org. Lett.*, 2014, **16**, 5776.

16 J. Wu, X. Wang, F. C. K. Chiu, C. Häberli, D. M. Shackleford, E. Ryan, S. Kamaraj, V. J. Bulbule, A. I. Wallick, Y. Dong, K. L. White, P. H. Davis, S. A. Charman, J. Keiser and J. L. Vennerstrom, *J. Med. Chem.*, 2020, **63**, 3723.

17 E. Y. Yamansarov, O. B. Kazakova, N. I. Medvedeva, D. V. Kazakov, O. S. Kukovinets and G. A. Tolstikov, *Russ. J. Org. Chem.*, 2014, **50**, 1043.

18 Y. Dong, J. Chollet, H. Matile, S. A. Charman, F. C. K. Chiu, W. N. Charman, B. Scorneaux, H. Urwyler, J. Santo Tomas, C. Scheurer, C. Snyder, A. Dorn, X. Wang, J. M. Karle, Y. Tang, S. Wittlin, R. Brun and J. L. Vennerstrom, *J. Med. Chem.*, 2005, **48**, 4953.

19 O. B. Kazakova, E. F. Khusnutdinova, A. V. Petrova, E. Y. Yamansarov, A. N. Lobov, A. A. Fedorova and K. Y. Suponitsky, *J. Nat. Prod.*, 2019, **82**, 2550.

20 R. Chhantyal-Pun, M. A. H. Khan, C. A. Taatjes, C. J. Percival, A. J. Orr-Ewing and D. E. Shallcross, *Int. Rev. Phys. Chem.*, 2020, **39**, 385.

21 B. R. Blank, R. L. Gonciarz, P. Talukder, J. Gut, J. Legac, P. J. Rosenthal and A. R. Renslo, *ACS Infect. Dis.*, 2020, **6**, 1827.

22 S. A. Charman, C. S. Perry, F. C. Chiu, K. A. McIntosh, R. J. Prankerd and W. N. Charman, *J. Pharm. Sci.*, 2006, **95**, 256.

23 E. M. W. Lauterwasser, S. D. Fontaine, H. Li, J. Gut, K. Katneni, S. A. Charman, P. J. Rosenthal, M. Bogyo and A. R. Renslo, *ACS Med. Chem. Lett.*, 2015, **6**, 1145.

24 P. S. Sijwali and P. J. Rosenthal, *Proc. Natl. Acad. Sci. U. S. A.*, 2004, **101**, 4384.

25 S. D. Fontaine, B. Spangler, J. Gut, E. M. Lauterwasser, P. J. Rosenthal and A. R. Renslo, *ChemMedChem*, 2015, **10**, 47.